

Original Research

# Inhibition of Galectin-3 Expression Could Preserve the Immunoregulatory Function of Mesenchymal Stem Cells During Cell Passaging

Minghui Wang<sup>1,†</sup>, Yan Jiang<sup>1,†</sup>, Jiangbo Wan<sup>1</sup>, Difan Zhang<sup>1</sup>, Fang Huang<sup>1,\*</sup>, Siguo Hao<sup>1,\*</sup>

Academic Editor: Amancio Carnero Mova

Submitted: 23 April 2025 Revised: 16 June 2025 Accepted: 7 August 2025 Published: 27 August 2025

#### Abstract

Background: Mesenchymal stem cells (MSCs) are one of the effective treatments for acute graft-versus-host disease (aGVHD) following allogeneic hematopoietic stem cell transplantation (allo-HSCT) due to their potent immunoregulatory function. Given the limited quantity and high heterogeneity of freshly isolated MSCs, extensive *in vitro* expansion is essential for clinical application. Prolonged passaging of MSCs leads to a decline in therapeutic efficacy, with the underlying mechanisms remaining unclear. This study aimed to explore the mechanism and intervention strategies of immunoregulatory dysfunction of MSCs during passaging. Methods: We compared the therapeutic effects of MSCs at early passages (passage 6, P6-MSCs) and later passages (passage 12, P12-MSCs) in a mouse GVHD model. We also analyzed the expression of Gal-3 in MSCs at different passages and its role in macrophage polarization. Additionally, the selective Gal-3 inhibitor TD139 was evaluated for its effects on Gal-3 expression and the immunoregulatory function of MSCs. Results: Our data showed an inverse correlation between passage number and therapeutic efficacy in MSCs. Late-passage MSCs (P12) exhibited significantly reduced efficacy in alleviating GVHD compared to early-passage MSCs (P6). The expression of Gal-3 was markedly upregulated in late-passage MSCs (P12), and it was found to directly inhibit anti-inflammatory M2-like macrophage polarization. Our research demonstrated that TD139 dose-dependently suppresses Gal-3 expression in MSCs and restores their immunoregulatory function. Conclusion: Gal-3 contributes to the decline in the immunomodulatory capabilities of MSCs. TD139, a Gal-3 inhibitor, has a potentially positive effect on rescuing the immunoregulation dysfunction of MSCs in late-passage and may represent a novel strategy to enhance the therapeutic potential of late-passage MSCs for GVHD treatment.

Keywords: mesenchymal stem cells; galectin-3; GB-0139 (TD139); graft vs host disease

### 1. Introduction

Allogeneic hematopoietic stem cell transplantation (allo-HSCT) is widely utilized for the treatment of various hematologic malignancies, demonstrating significant immunotherapeutic potential [1]. However, it is constrained by severe graft-versus-host-disease (GVHD), which is a life-threatening complication [2]. The conditioning regimen in allo-HSCT activates antigen-presenting cells (APCs)—predominantly macrophages and dendritic cells—that present host antigens to donor T cells and initiate a robust cytokine response. Effector T cells, macrophages and pro-inflammatory cytokines target skin, lungs, gut and liver, leading to organ damage, which is a clinical manifestation of aGVHD [3].

Mesenchymal stem cells (MSCs) represent a unique population of multipotent precursor cells, defined by their capacities for self-renewal and differentiation into a range of cell lineages, including chondrocytes, osteoblasts, adipocytes, cardiomyocytes, and neurons [4,5]. Furthermore, MSCs exhibit potent immunoregulatory properties,

modulating both innate and adaptive immune responses. This immunoregulatory effect is primarily induced by inflammatory cytokines within the inflammatory microenvironment [6,7]. MSCs have been demonstrated to facilitate the shift of macrophages from the pro-inflammatory M1 phenotype to the anti-inflammatory M2 phenotype, while simultaneously inhibiting macrophage infiltration at inflammatory sites [8]. Additionally, MSCs directly inhibit the activation of cytotoxic CD8<sup>+</sup> T cells and the differentiation of T helper 1 (Th1) and Th17 cells [9]. Simultaneously, they facilitate the differentiation and activity of CD4<sup>+</sup>CD25<sup>+</sup>FOXP3<sup>+</sup> Treg cells [10,11]. This combined capacity for self-renewal and multilineage differentiation, coupled with their immunoregulatory function, underscores the potential of MSCs as a viable therapeutic modality.

MSCs are isolatable from a range of tissue sources, including bone marrow, adipose tissue, umbilical cord, and peripheral blood [12,13]. Given the limited abundance of MSCs in these tissues, extensive *ex vivo* expansion is required to achieve the sufficient cell numbers necessary for

<sup>&</sup>lt;sup>1</sup>Department of Hematology, Xinhua Hospital Affiliated to Shanghai Jiao Tong University School of Medicine, 200090 Shanghai, China

<sup>\*</sup>Correspondence: huangfang335@163.com (Fang Huang); haosiguo@xinhuamed.com.cn (Siguo Hao)

<sup>&</sup>lt;sup>†</sup>These authors contributed equally.

*in vivo* application [14]. However, multiple studies have shown that MSCs may undergo a decline in their immunosuppressive and regenerative capacities after extended passages [15–18].

Galectin-3 (Gal-3, gene name: Lgals3), a  $\beta$ -galactoside-binding lectin, is widely expressed in various tissues and by most cell types, emerging as a crucial factor in processes such as cell proliferation, apoptosis, inflammation, and fibrosis. It exerts regulatory effects on both chronic and acute inflammatory conditions across different tissues [19,20]. Several investigations have revealed that Gal-3 exerts a notable influence on pro-inflammatory processes by inhibiting M2 macrophage polarization [21–23]. Furthermore, downregulation of Gal-3 has been shown to attenuate inflammation [24]. It has been shown that Gal-3 suppresses T cell activation by inhibitory receptors that negatively regulate T cell activation and responses [25].

Selective galectin inhibitors (TAZTDG, TD139, GB0139) modulate multiple pathophysiological processes, demonstrating significant potential as therapeutic candidates [26]. Among them, TD139 is a small-molecule inhibitor that selectively targets Gal3 by disrupting its  $\beta$ -galactoside-binding activity [27]. This compound has demonstrated efficacy in preclinical models of fibrosis and inflammation and is currently being evaluated in Phase II clinical trials for idiopathic pulmonary fibrosis and platelet activation [28–30].

Macrophages constitute a vital element of the innate immune system and mediate critical functions in both inflammatory responses and host defense [31]. In response to differing microenvironments, macrophages adopt distinct functional phenotypes: classically activated macrophages (M1-like) and alternatively activated macrophages (M2-like) [32]. M1-like macrophages are activated by lipopolysaccharide (LPS), resulting in the release of pro-inflammatory cytokines. These macrophages primarily mediate inflammatory responses and contribute to tissue damage. In contrast, M2-like macrophages are activated by interleukin-4 (IL-4), triggering the secretion of anti-inflammatory cytokines. These macrophages predominantly participate in anti-inflammatory responses and tissue repair [33].

The precise mechanism underlying the decline in the immunoregulatory effects of MSCs after multiple passages remains to be elucidated and constituted the primary focus of this study. Our results demonstrated that the effect of late-passage MSCs on M2-like macrophage polarization was diminished both *in vivo* and *in vitro*. Additionally, Galectin-3 (Gal-3) was significantly upregulated in late-passage MSCs compared to early-passage MSCs. Furthermore, Gal-3 directly inhibited M2-like macrophage polarization. Therefore, we hypothesized that the attenuation of the immunoregulatory function of MSCs was attributed to the overexpression of Gal-3 in late-passage MSCs. Notably, TD139, a selective Gal-3 inhibitor, dose-dependently

suppressed Gal-3 expression in MSCs, particularly in latepassage MSCs. More importantly, TD139 enhances the immunoregulatory potential of late-passage MSCs by promoting M2 macrophage polarization. Based on these findings, the combination of TD139 and MSCs may represent a novel therapeutic strategy for GVHD and other diseases.

### 2. Materials and Methods

#### 2.1 Reagents and Animals

Fetal bovine serum (FBS), penicillin-streptomycin (P/S), trypsin-ethylenediaminetetraacetic acid (EDTA) were purchased from Gibco (Grand Island, NY, USA). CD4 and CD8 MicroBeads and the AutoMACS system were purchased from Miltenyi Biotec. (Shanghai, China). Biolegend (San Diego, CA, USA) -provided antibodies included: APC-conjugated CD29 (303008), CD19 (115512), and F4/80 (123115); PE-conjugated CD11c (117307), Sca1 (108107), CD206 (141705), and inducible nitric oxide synthase (iNOS) (696805); with PE-Cy7-CD44 (103029) and FITC-CD11b (101205). Hieff qPCR SYBR Green Master Mix was acquired from Yeasen (Shanghai, China). FOXP3/Transcription Factor Staining Buffer set was purchased from eBioscience (San Diego, CA, USA). All primers were obtained from Sangon Biotech (Shanghai, China). TD139, Galectin-3 were purchased from Selleck&Bimake (Selleck&Bimake, Shanghai, China).

Male BALB/c (H-2d) and C57BL/6 (H-2b) mice (10–12 weeks old) were obtained from Shanghai Laboratory Animal Center (SLAC, Shanghai, China) and maintained in specific pathogen-free (SPF) conditions with autoclaved water and standard chow. All animal tests were conducted in compliance with the guidelines established by the Ethics Committee of Xinhua Hospital Affiliated with the Shanghai Jiao Tong University School of Medicine (Ethics Approval No. XHEC-F-2022-076). All mice in this study were euthanized by cervical dislocation, in strict accordance with the guidelines outlined by the Ethics Committee of Xinhua Hospital Affiliated with the Shanghai Jiao Tong University School of Medicine (Shanghai, China).

### 2.2 Cell Culture

MSCs isolated from bone marrow of C57BL/6 mice were cultured in Dulbecco modified Eagle medium-low glucose (DMEM-L; Hyclone, Shanghai, China) containing 10% heat-inactivated fetal bovine serum (FBS; Gibco, USA) and 1% penicillin-streptomycin (10,000 U/mL penicillin, 10,000 µg/mL streptomycin) (1% P/S; Gibco, USA) at 37 °C in a humidified atmosphere of 5% CO2. MSCs at passage 2 (P2- MSCs) were passaged by 0.25% trypsinethylenediaminetetraacetic acid (EDTA; Gibco, Burlington, Canada) at a 1:3 ratio when they were 80%–90% confluent, up to P12. Here, the MSCs were classified as early passages of MSCs (passage 4 to 6-MSCs) and late passages (passage 7 to 12-MSCs). MSCs exhibited typical fibroblast-like morphology, characterized by long, polyg-



Table 1. Sequences of primers designed to measure the gene expression by qRT-PCR from MSCs or Raw 264.7 cells.

Gene	Forward Primers (5'-3')	Reverse Primers (5'-3')
β-actin	CATTGCTGACAGGATGCAGAAGG	TGCTGGAAGGTGACAGTGAGG
Galectin-3 (LGALS3)	AGACAGCTTTTCGCTTAACGA	GGGTAGGCACTAGGAGGAGC
$TGF$ - $\beta 1$	CTCCCGTGGCTTCTAGTGC	GCCTTAGTTTGGACAGGATCTG
IL-10	GCTCTTACTGACTGGCATGAG	CGCAGCTCTAGGAGCATGTG
Arg	AGCACTGAGGAAAGCTGGTC	TACGTCTCGCAAGCCAATGT
Ym1	CAGGTCTGGCAATTCTTCTGAA	GTCTTGCTCATGTGTGTAAGTGA
CD206 (MR)	AAACACAGACTGACCCTTCCC	GTTAGTGTACCGCACCCTCC
$IL$ -1 $\beta$	GTCACAAGAAACCATGGCACAT	GCCCATCAGAGGCAAGGA
IL-6	GAACAACGATGATGCACTTGC	CTTCATGTACTCCAGGTAGCTATGGT
$TNF$ - $\alpha$	CTTCTGTCTACTGAACTTCGGG	CACTTGGTGGTTTGCTACGAC
COX2	GCCTACTACAAGTGTTTCTTTTTGCA	CATTTTGTTTGATTGTTCACACCAT
CCL2	AGGTGTCCCAAAGAAGCTGTA	ATGTCTGGACCCATTCCTTCT
CCL3	TGACACTCTGCAACCAAGTCTTC	AACGATGAATTGGCGTGGAA
CCL4	TTCTCTTACACCTCCCGGCAG	GTACTCAGTGACCCAGGGCTCA
iNOS	CAGCTGGGCTGTACAAACCTT	CATTGGAAGTGAAGCGTTTCG
Galectin-1 (Lgals1)	AACCTGGGGAATGTCTCAAAGT	GGTGATGCACACCTCTGTGA

qRT-PCR, Quantitative Real-time PCR; MSCs, Mesenchymal stem cells; TGF- $\beta I$ , Transforming growth factor-beta1; IL-I0, interleukin-10; Arg, Arginase; IL- $I\beta$ , interleukin-1beta; IL-6, interleukin-6; TNF- $\alpha$ , Tumor necrosis factor- $\alpha$ ; COX2, cyclooxygenase 2; CCL2, CC-chemokine ligand 2; CCL3, CC-chemokine ligand 3; CCL4, CC-chemokine ligand 4; iNOS, inducible nitric oxide synthase.

onal, plastic-adherent cells, and display the typical immunophenotypes, including Sca1 (+), CD29 (+), CD44 (+), CD19 (-), and CD11b (-) (**Supplementary Fig. 1A,B**).

The Raw264.7 cells, a macrophage cell line, were purchased from the American Type Culture Collection (Manassas, VA, USA). Cells were cultured in Dulbecco modified Eagle medium glucose (DMEM; Hyclone, China) containing 10% FBS and 1% P/S at 37 °C in a humidified atmosphere of 5% CO<sub>2</sub>.

All cell lines (including Raw264.7) were validated by STR profiling and tested negative for mycoplasma contamination.

### 2.3 Quantitative Real-time PCR (qRT-PCR)

Firstly, total RNA was extracted from cells using EZ-press RNA Purification Kit (EZBioscience, CA, USA) according to manufacturer's protocol. Total RNA meeting purity criteria (A260/A280 ratio 1.8–2.0) was converted to complementary deoxyribonucleic acid (cDNA) with PrimerScript<sup>TM</sup> RT Master Mix (Takara, Shiga, Japan) per manufacturer's instructions. qRT-PCR was performed using relevant gene-specific primers and Hieff qPCR SYBR Green Master Mix (Yeasen, China) on Step One Plus Realtime PCR System (Life Technologies, CA, USA). The messenger ribonucleic acid (mRNA) expression levels of target genes were normalized to  $\beta$ -actin gene and calculated according to the  $2^{-\Delta\Delta CT}$  method. All primers were obtained from Sangon Biotech. Primer sequences are shown in Table 1.

### 2.4 Flow Cytometry Analysis

Fluorescein conjugated monoclonal (mAbs) used for experiments include phycoerythrin (PE)conjugated mAbs to mouse, Fluorescein isothiocyanate (FITC)-conjugated mAbs to mouse, allophycocyanin (APC)-conjugated mAbs to mouse and R-Phycoerythrin-Cyanine 7 (PE-Cy7)-conjugated mAbs to mouse. Antibody information are provided in the Reagents and Animals section. In brief, for cell surface antigen staining, cells were collected, washed with phosphate buffered solution (PBS) and incubated with relevant fluorescein-conjugated mAb in the dark for 30 minutes at 4 °C. For cell nuclear/intracellular antigen staining, after stained with cell surface antigen, cells were fixed and permeabilized with eBioscience™ FOXP3/Transcription Factor Staining Buffer set (Invitrogen, CA, USA) according to the manufacture's protocol followed by intracellular staining with relevant fluorescein-conjugated mAb in the dark for 30 minutes at room temperature. Finally, cells were washed with PBS and performed flow cytometric analysis. Flow cytometry (FCM) was performed by using BD FACS CantoII (Becton-Dickinson Bioscience, Franklin Lakes, NJ, USA) and analysis was performed by using FlowJo software (Version 10.8.1; BD Biosciences, Ashland, OR, USA).

# 2.5 Establishment and Assessment of Acute GVHD Mice Model

Mice underwent bone marrow (BM) transplantation (BMT) according to the protocol described previously [34]. Briefly, recipient mice (BALB/c, male, 10–12 weeks) were



randomly divided into three groups as follows: the T cell depleted-bone marrow cells (TCD-BMC) + T cells + vehicle group, the TCD-BMC + T cells + P6-MSCs group and the TCD-BMC + T cells + P12-MSCs group. At day 0, after BALB/c recipients received 7.0 Gy (137Cesium source at 100 cGy/min) total body irradiation (TBI), TCD-BMC (5  $\times$  10<sup>6</sup> cells/mouse) together with splenic CD3<sup>+</sup> T cells (2  $\times$  10<sup>6</sup> cells/mouse) from allogeneic donor mice (C57BL/6) were collected and co-injected into BALB/c recipients via tail vain. The recipients were transfused with vehicle, P6-MSCs (3  $\times$  10<sup>5</sup> cells/mouse) or P12-MSCs (3  $\times$  10<sup>5</sup> cells/mouse) intravenously at day 1, 3, 5 according to groups they were assigned to. The severity of GVHD was evaluated every 2 days post-transplantation using a standardized clinical scoring system, based on five parameters: weight loss, posture, activity, fur texture, and skin integrity. Scoring criteria conformed to established protocols as previously described [35]. The mice were euthanized via cervical dislocation on day 21 post-TBI without prior anesthesia, following which peritoneal cavityderived macrophages were collected for subsequent analysis. Target organs (liver, lung, small intestine) were collected from per experimental group, fixed in 10% formalin, paraffin-embedded, hematoxylin and eosin (H&E)-stained, and blindly evaluated for GVHD pathology.

### 2.6 Isolation of T-cells

Spleens harvested from C57BL/6 mice were grinded through 40-µm nylon cell strainers and obtained splenic cell suspension. CD4+/CD8+ T cell isolation or depletion was performed using CD4 and CD8a MicroBeads and the AutoMACS system (Miltenyi Biotec, Germany) according to the manufacturer's protocol. Briefly, 10 µL of CD4 MicroBeads and 10 µL of CD8a MicroBeads were added per  $1\times10^7$  cells, and the mixture was incubated for 15 minutes at 4 °C in the dark. The cell suspension was then passed through a pre-rinsed LS column mounted on the AutoMACS Pro Separator to retain T cells (CD4+ and CD8+) via magnetic separation.

### 2.7 Generation of T Cell Depleted-bone Marrow Cells

Bone marrow cells (BMC) were isolated from the femurs and tibias of C57BL/6 mice following humane euthanasia. The marrow cavity was flushed with ice-cold DMEM-complete medium using a 25-gauge needle to obtain a single-cell suspension, which was sequentially filtered through a 40- $\mu$ m nylon cell strainer to remove debris. Red blood cells in the suspension were lysed with ACK lysis buffer, and the resulting nucleated cell pellet was resuspended in MACS Buffer at a concentration of 1  $\times$  10<sup>8</sup> cells/mL. T cell depletion (TCD) was performed using CD4 and CD8a MicroBeads according to the manufacturer's protocol. The efficiency of T cell depletion was validated by flow cytometry using anti-mouse CD3-PE antibody. Only TCD-BMC preparations with residual CD3<sup>+</sup> T cells  $\leq$ 1%

(consistent with purity validation in **Supplementary Fig.** 2) were used for transplantation experiments.

### 2.8 Preparation and Analysis of Macrophages

Macrophages were harvested from the peritoneal lavage of recipient mice at day 21 after BMT. After intraperitoneal injection of pre-cooled PBS, gentle abdominal massage was performed prior to peritoneal lavage fluid collection. Finally, the harvested cells were stained for flow cytometric analysis using anti-mouse CD11b-FITC, anti-mouse F4/80-APC and anti-mouse CD206-PE and anti-mouse iNOS-PE antibodies. CD11b+F4/80+ double-positive cells were identified as peritoneal macrophages (Supplementary Fig. 3).

### 2.9 Effects of MSCs on Macrophages

To investigate the effects of MSCs on macrophages at different passages, P6-MSCs and P12-MSCs were seeded into the lower chamber of transwell (Corning, USA, catalog number 3412, pore diameter 0.4  $\mu m$ , polycarbonate membrane) at a density of 2  $\times$  10<sup>5</sup> per well. When they reached approximately 70% confluence, Raw 264.7 cells were seeded into the upper chamber of transwell at a density of 1  $\times$  10<sup>7</sup> per well and co-cultured with P6-MSCs or P12-MSCs for 48 hours. Besides, the co-culture system was treated with vehicle, Gal-3 (500 ng/mL), TD139 (100  $\mu M$ ), LPS (100 ng/mL) + vehicle, LPS (100 ng/mL) + galectin-3 (500 ng/mL), or LPS (100 ng/mL) + TD139 (100  $\mu M$ ). Finally, Raw264.7 cells were collected and stained with PEconjugated anti-mouse CD206 or iNOS antibodies for flow cytometry.

# 2.10 Effects of Gal-3 on Macrophages

Raw264.7 cells were seeded into 24-well plates at a density of  $3 \times 10^6$  per well and treated with vehicle, galectin-3 (100 ng/mL), galectin-3 (500 ng/mL) for 48 hours. Galectin-3 was dissolved in ddH<sub>2</sub>O. Raw264.7 cells were collected and stained with anti-mouse CD206-PE or anti-mouse iNOS-PE antibodies for flow cytometry. Besides, expression of macrophage polarization-related mediator (iNOS, interleukin-1beta (IL-1 $\beta$ ), interleukin-6 (IL-6), Tumor necrosis factor- $\alpha$  (TNF- $\alpha$ ), CC-chemokine ligand 2 (CCL2), CC-chemokine ligand 3 (CCL3), CC-chemokine ligand 4 (CCL4), cyclooxygenase 2 (COX2), interleukin-10 (IL-10), YM1, Transforming growth factor-beta1 (TGF- $\beta$ 1), Arginase (Arg) and CD206) in Raw264.7 cells were determined by qPCR across experimental groups.

#### 2.11 Cell Proliferation Assay

MSCs at different passages were seeded in 96-well cell culture plates at  $3\times10^3$  per well. The cells were treated with vehicle or TD139 at 100  $\mu$ M concentration for 72 h. The absorbance at 450 nm was measured every 24 h with a microplate reader (Thermo Fisher) according to the instructions of the CCK-8 kit (cell counting kit-8, Beyotime,



China). The total numbers of migrated cells were counted to evaluate cell proliferation.

### 2.12 Effects of TD139 on Macrophages

Raw 264.7 macrophages were seeded in 24-well cell culture plates at  $1.5\times10^6$  per well. TD139 was dissolved in DMSO. The cells were treated with vehicle or TD139 (100  $\mu M)$  for 48 h. Then, the Raw 264.7 macrophages were harvested and stained for flow cytometric analysis using antimouse CD206-PE or anti-mouse iNOS-PE antibodies.

### 2.13 Statistical Analysis

All experiments were independently repeated a minimum of two to three times. The figure legends provide detailed information on reproducibility and sample sizes. Data are presented as mean  $\pm$  standard deviation. Statistical analyses were performed using one-way or two-way analysis of variance (ANOVA) or Student's *t*-test with GraphPad Prism software. Non-parametric murine survival data were analyzed using the log-rank test. All *p* values were two-sided, with p < 0.05 considered statistically significant.

### 3. Results

# 3.1 Late-passage MSCs Poorly Alleviated the Severity of GVHD

To determine whether passage number of MSCs would affects the therapeutic efficacy of MSCs in GVHD, recipient mice were received MSCs at different passages after BMT (Fig. 1A). Although there were no significant differences in survival of mice among three groups (Fig. 1B), the clinical GVHD scores were significantly higher in recipients treated with P12-MSCs compared to those treated with P6-MSCs (Fig. 1C, p < 0.0001). To confirm these results, histopathological examination was performed at day 21 post-BMT. As shown in Fig. 1D, the histopathological images showed more severe tissue damage in GVHD-target organs including small intestine, liver, lungs, in P12-MSCstreated recipients compared to those treated with P6-MSCs. Taken together, these results suggest that MSCs at late passage (P12) are less effective in alleviating the severity of acute GVHD (aGVHD) compared to MSCs at early passage

# 3.2 The Effect of Late-passage MSCs (P12) on M2-like Macrophages Polarization was Weakened

Next, we sought to explore the potential mechanisms underlying the variation in MSCs at different passages in the context of GVHD. Given the powerful immunoregulatory effects of MSCs on macrophages, we next assessed the polarization of macrophages isolated from peritoneal lavage liquid of GVHD mice model treated with MSCs at different passages. Compared to the P6-MSCs-treated mice, the proportion of F4/80 $^+$  CD11b $^+$  CD206 $^+$  M2-like macrophages was lower in the P12-MSCs-treated mice (Fig. 2A, p < 0.0001). Meanwhile, we utilized Raw246.7

cell line to investigate the effects of MSCs at different passages on macrophages *in vitro*. After co-culturing with MSCs at different passages, the proportion of CD206<sup>+</sup> M2-like macrophages was also lower in P12-MSCs-treated group than that in P6-MSCs-treated group (Fig. 2B, p < 0.05). Moreover, the proportion of iNOS<sup>+</sup> M1-like macrophages in Raw264.7 cells was higher in P12-MSCs-treated group than in P6-MSCs-treated group (data not shown). Collectively, our results indicated that MSCs at later passages exhibit a significantly reduced ability to induce M2 macrophage polarization.

To simulate the in vivo inflammatory environment, we supplemented the MSCs-Raw264.7 macrophage co-culture system with LPS. Although the proportion of CD206<sup>+</sup> M2-like macrophages and iNOS+ M1-like macrophages did not differ significantly between P6-MSCs-treated and P12-MSCs-treated groups, mRNA expression of M2associated anti-inflammatory mediators, such as IL-10 was reduced, while the mRNA expression of M1-associated pro-inflammatory mediators, including L-6, CCL4, and COX2, was elevated in the P12-MSCs-treated group compared to the P6-MSCs-treated group (Fig. 3A,B). Our results indicated that the therapeutic efficacy of MSCs at different passages for acute GVHD could be related to macrophage polarization and the effect of MSCs at late passage on M2-like macrophages polarization was notably weakened.

# 3.3 Galectin-3 Directly Suppressed M2-like Macrophages Polarization

Previous studies have demonstrated that the activation of Gal-3 enhances inflammation [23], whereas the downregulation of Gal-3 can suppress inflammatory responses [24]. Several studies have indicated that Gal-3 promotes a pro-inflammatory response by inhibiting M2 macrophage polarization and inducing apoptosis [21,22]. MSCs constitutively express Gal-3 at both the mRNA and protein levels, thereby exerting immunomodulatory effect via galectins [36]. Moreover, Gal-3 is a new informative model to predict aGVHD development [37]. Based on this, we inferred that Gal-3 expression may be linked to the effects of MSCs on macrophages, to verify this point, we first analyzed the expression of Gal-3 in MSCs at different passages. As shown in Fig. 4, Gal-3 expression escalated starting at passage10 and markedly higher in MSCs at later passages compared to those at earlier passages. Then, we assessed the characteristics of Raw 264.7 macrophages in the presence of Gal-3. As shown in Fig. 5A, the proportion of iNOS<sup>+</sup> M1-like macrophages notably increased in Gal-3-treated Raw 264.7 cells in a dosedependent manner after 48 h. The M1-like macrophage phenotype is characterized by the expression of chemokines such as iNOS, CCL2, CCL3, CCL4 and the induction of pro-inflammatory mediators including IL-1β, IL-6, TNF- $\alpha$ , COX2. Our data showed that, in addition to IL-1 $\beta$ ,



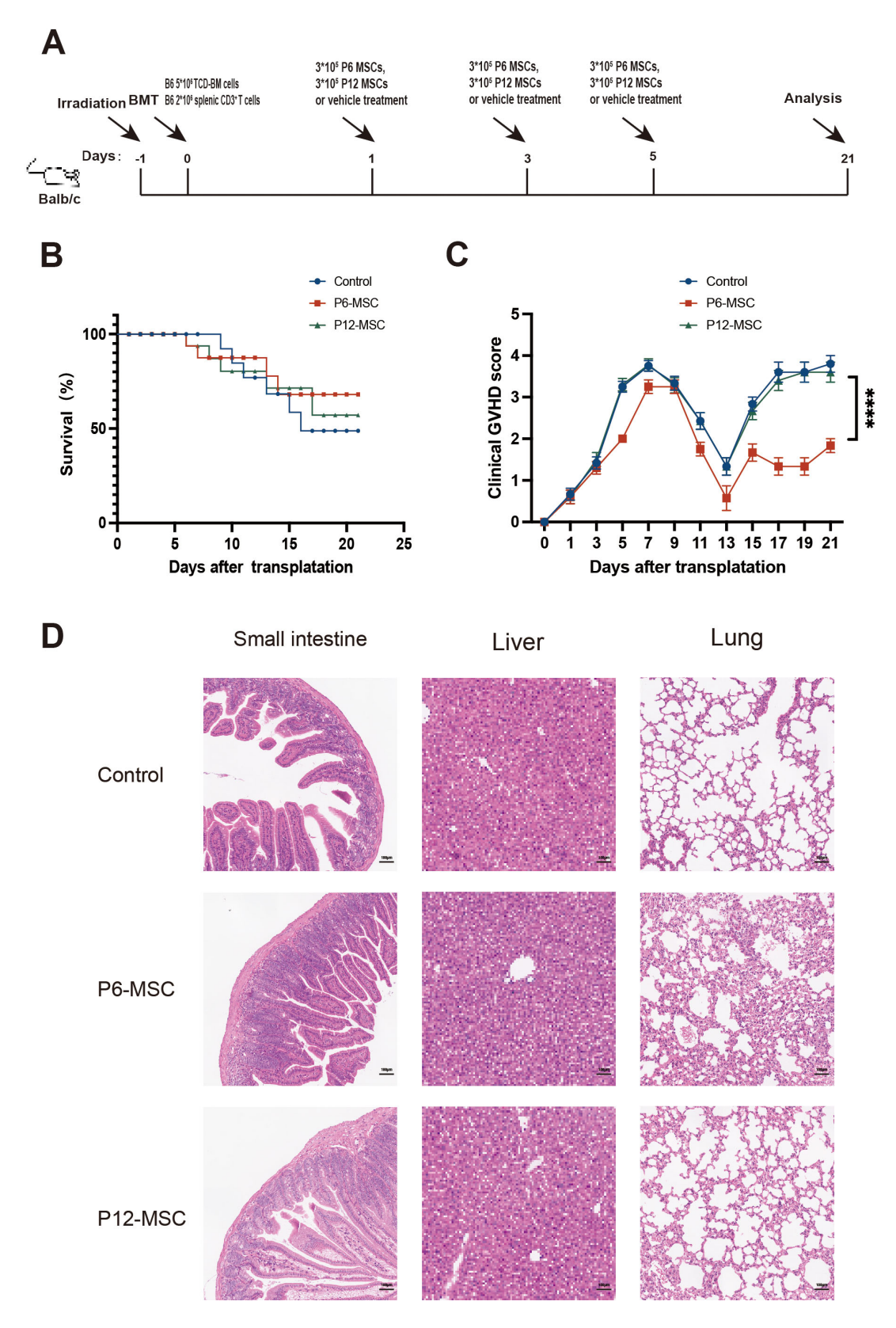


Fig. 1. Effects of MSCs at different passages on the GVHD mice. (A) Experimental scheme for GVHD model establishment and treatment. (B) Kaplan-Meier survival curve of GVHD mice treated with PBS, P6-MSCs, P12-MSCs. (C) Clinical GVHD score of GVHD mice treated with PBS, P6-MSCs, P12-MSCs. (D) Representative histopathology images of liver, lung and small intestine from GVHD mice treated with PBS, P6-MSC and P12-MSC on day 21 after transplantation. Scale bar, 100  $\mu$ m. Data were pooled from 3 independent experiments. N = 3–5 in each group. \*\*\*\*p < 0.0001. GVHD, graft-versus-host-disease; PBS, phosphate buffered solution.

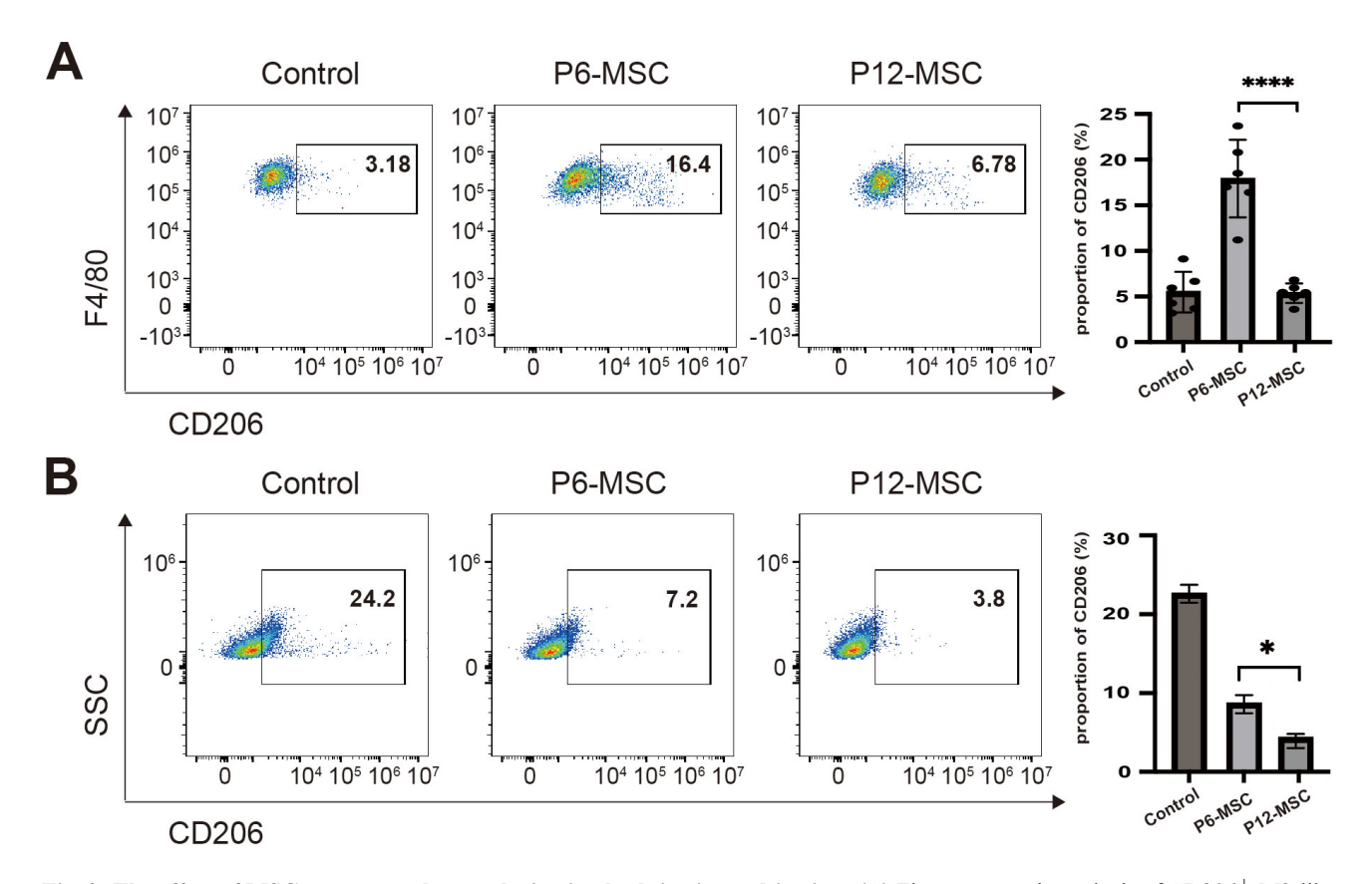


Fig. 2. The effect of MSCs on macrophage polarization both *in vivo* and *in vitro*. (A) Flow cytometric analysis of CD206<sup>+</sup> M2-like macrophage proportion within F4/80<sup>+</sup>CD11b<sup>+</sup> peritoneal macrophages from GVHD mice treated with PBS, P6-MSCs or P12-MSCs on day 21 post-transplantation. (B) Flow cytometric analysis of CD206<sup>+</sup> M2-like macrophages percentages in Raw264.7 cells co-cultured with vehicle control (culture medium alone), P6-MSCs, or P12-MSCs without LPS stimulation for 48 hours. Data were pooled from 3 independent experiments. \*p < 0.05, \*\*\*\*p < 0.0001. LPS, lipopolysaccharide.

the mRNA expression of these M1-associated mediators was significantly upregulated in Raw 264.7 macrophages treated with high doses of Gal-3 (Fig. 5B, p < 0.01). Furthermore, the proportion of CD206<sup>+</sup> M2-like macrophages in Gal-3 treated group was significant decreased in a dosedependent manner compared to the control groups (Fig. 5C, p < 0.01). Meanwhile, anti-inflammatory mediators associated with the M2 macrophage phenotype, including IL-10, TGF-β1, Arg, and Ym1, were decreased in Gal-3-treated Raw264.7 macrophages compared to the control groups (Fig. 5D, p < 0.0001). All these data suggested that the differential effects of MSCs at different passages on macrophage polarization may be related to Gal-3. As MSCs progress through passages, they express higher levels of Gal-3, which could concentration-dependently induce macrophage polarization toward the iNOS<sup>+</sup> M1 phenotype while suppressing CD206<sup>+</sup> M2 macrophage polarization.

# 3.4 TD139 Could Suppress Gal-3 Expression in MSCs and Save the Immunoregulatory Function of MSCs at Later Passages

Based on the above data, it is evident that elevated expression of Gal-3 in MSCs at later passages results in

a diminished effect of MSCs on M2-like macrophage polarization. In this study, we sought to assess the potential applications of Gal-3 inhibitors. While prior studies have focused on Gal-3, our data demonstrated that Gal-1 is also expressed in MSC (Supplementary Fig. 4A). TD139, a selective small-molecule inhibitor of Gal-3, with no impact on Gal-1 (Supplementary Fig. 4B), and is currently undergoing Phase II clinical trials for idiopathic pulmonary fibrosis [28,38]. Treatment with TD139 at concentrations ranging from 10-100 µM for 48 hours led to a significant dose-dependent reduction of Gal-3 expression in P12-MSCs (Fig. 6A). Based on this observation, a concentration of 100 µM TD139 was selected for subsequent experiments. Similarly, Gal-3 expression was also inhibited in P6-MSCs following high-dose TD139 treatment (Fig. 6B, p < 0.0001). In addition, our data showed that TD139 treatment did not alter MSCs proliferation and viability (Supplementary Fig. 5).

To determine whether TD139 affect other profiles of MSCs, we also examined the immunophenotype of MSCs in presence of TD139. The results revealed that MSCs cultured with or without TD139 exhibited typical fibroblast-like morphology, characterized by long, polygonal, plastic-



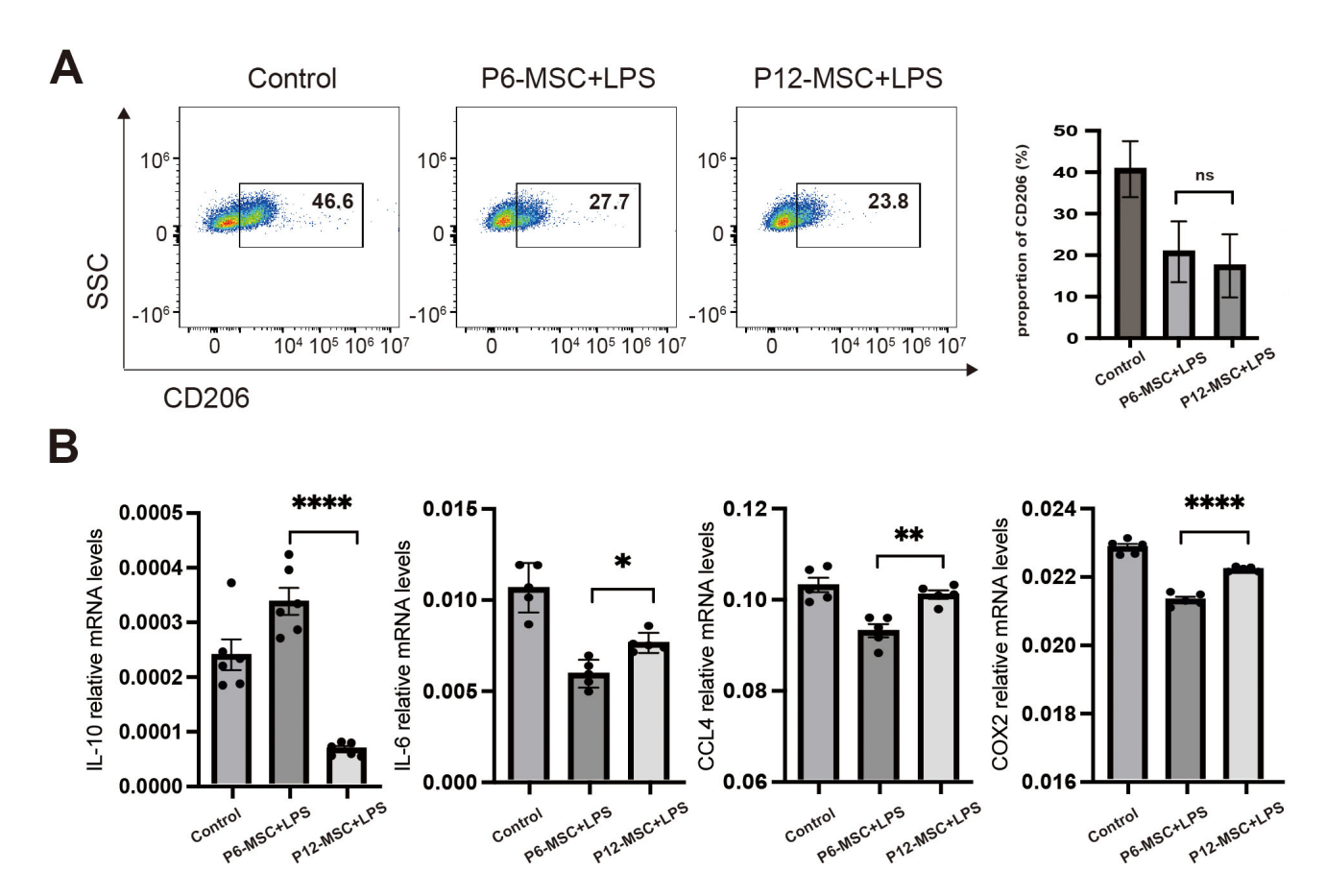


Fig. 3. The effect of MSCs on macrophage polarization in the present of LPS. Raw264.7 cells were cocultured with vehicle control (culture medium alone), P6-MSCs or P12-MSCs in the present of 100 ng/mL LPS for 48 h, distinct from Fig. 2 (no LPS). (A) Flow cytometric analysis of CD206<sup>+</sup> cell percentages in Raw264.7 macrophages. (B) qPCR analysis of macrophage polarization-related mediator expression (IL-10, IL-6, CCL4, and COX2) in Raw264.7 macrophages. Data were pooled from 3 independent experiments. Data are presented as the mean  $\pm$  SD. ns (p > 0.05), \*p < 0.05, \*\*p < 0.01, \*\*\*\*p < 0.001. SSC, Side Scatter.

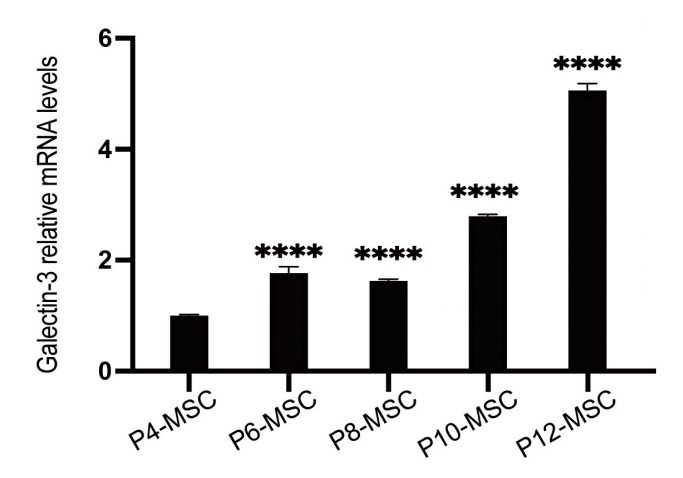


Fig. 4. The mRNA expression of Galectin-3 in MSCs at different passages by qPCR. Data were pooled from 3 independent experiments. Data are presented as the mean  $\pm$  SD. \*\*\*\*p < 0.0001.

adherent cells, and displayed the expected immunophenotypes of MSCs, including Sca1 (+), CD29 (+), CD44 (-), CD19 (-), and CD11b (-) (data not shown). These find-

ings indicated that TD139 effectively inhibits Gal-3 expression in MSCs without altering their fundamental biological properties, including morphology and immunophenotype.

Since TD139 inhibits Gal-3 expression in MSCs, we inferred that TD139 could improve the immunoregulatory function of MSCs. In this study, we investigated the impact of TD139 on macrophage polarization induced by MSCs. As shown in Fig. 6, after incubation with TD139 at a concentration of 100 μM, the proportion of CD206<sup>+</sup> M2-like macrophages relative to Raw264.7 macrophages was significantly increased in the TD139-treated P6-MSCs group compared to the vehicle-treated P6-MSCs group (Fig. 6C, p < 0.05). Besides, the proportion of CD206<sup>+</sup> M2-like macrophages relative to Raw264.7 macrophages was also increased in the TD139-treated P12-MSCs group compared to the vehicle-treated P12-MSCs group (Fig. 6D, p < 0.001). Moreover, although no significant differences were observed among groups containing P6-MSCs, the percentage of iNOS+ M1-like macrophages was decreased in the TD139-treated P12-MSCs group compared to the vehicle-treated P12-MSCs group (data not shown). Taken together, these results demonstrated that TD139



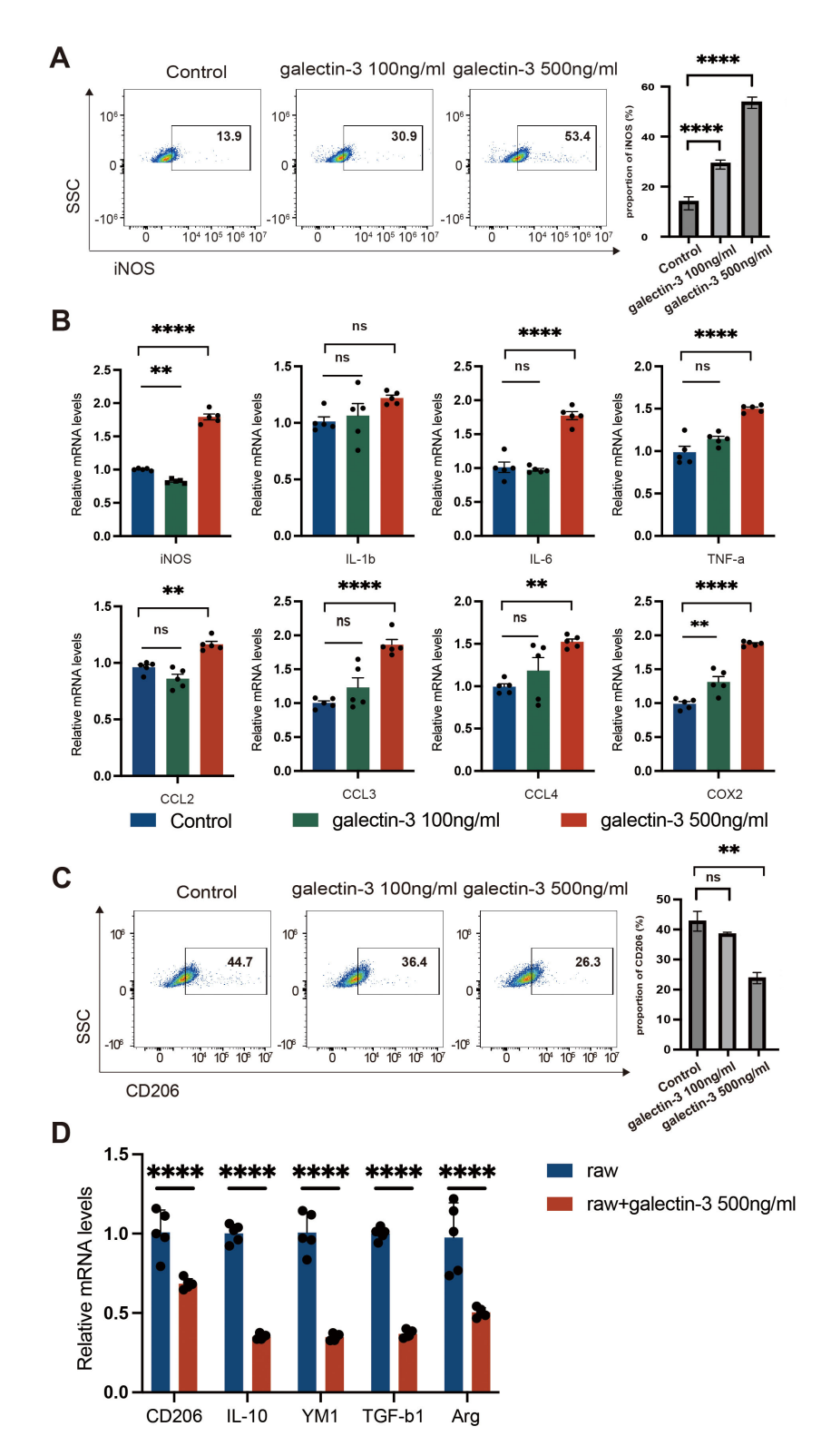


Fig. 5. The effect of Gal-3 on macrophage polarization. Raw264.7 cells were treated with vehicle, Gal-3 (100 ng/mL) or Gal-3 (500 ng/mL) for 48 h. (A) Flow cytometry analysis of iNOS<sup>+</sup> M1 macrophage proportion in Raw264.7 macrophages. (B) qPCR analysis of iNOS<sup>+</sup> M1 macrophage polarization-related mediator expression (iNOS, IL-1 $\beta$ , IL-6, TNF- $\alpha$ , CCL2, CCL3, CCL4 and COX2) in Raw264.7 macrophages. (C) Flow cytometry analysis of CD206<sup>+</sup> M2 macrophage proportion in Raw264.7 macrophages. (D) qPCR analysis of CD206<sup>+</sup> M2 macrophage polarization-related mediator expression (IL-10, YM1, TGF- $\beta$ 1, Arg and CD206) in Raw264.7 macrophages. Data were pooled from 3 independent experiments. Data are presented as the mean  $\pm$  SD. ns (p > 0.05), \*\*p < 0.01, \*\*\*\*p < 0.0001. Gal-3, Galectin-3.

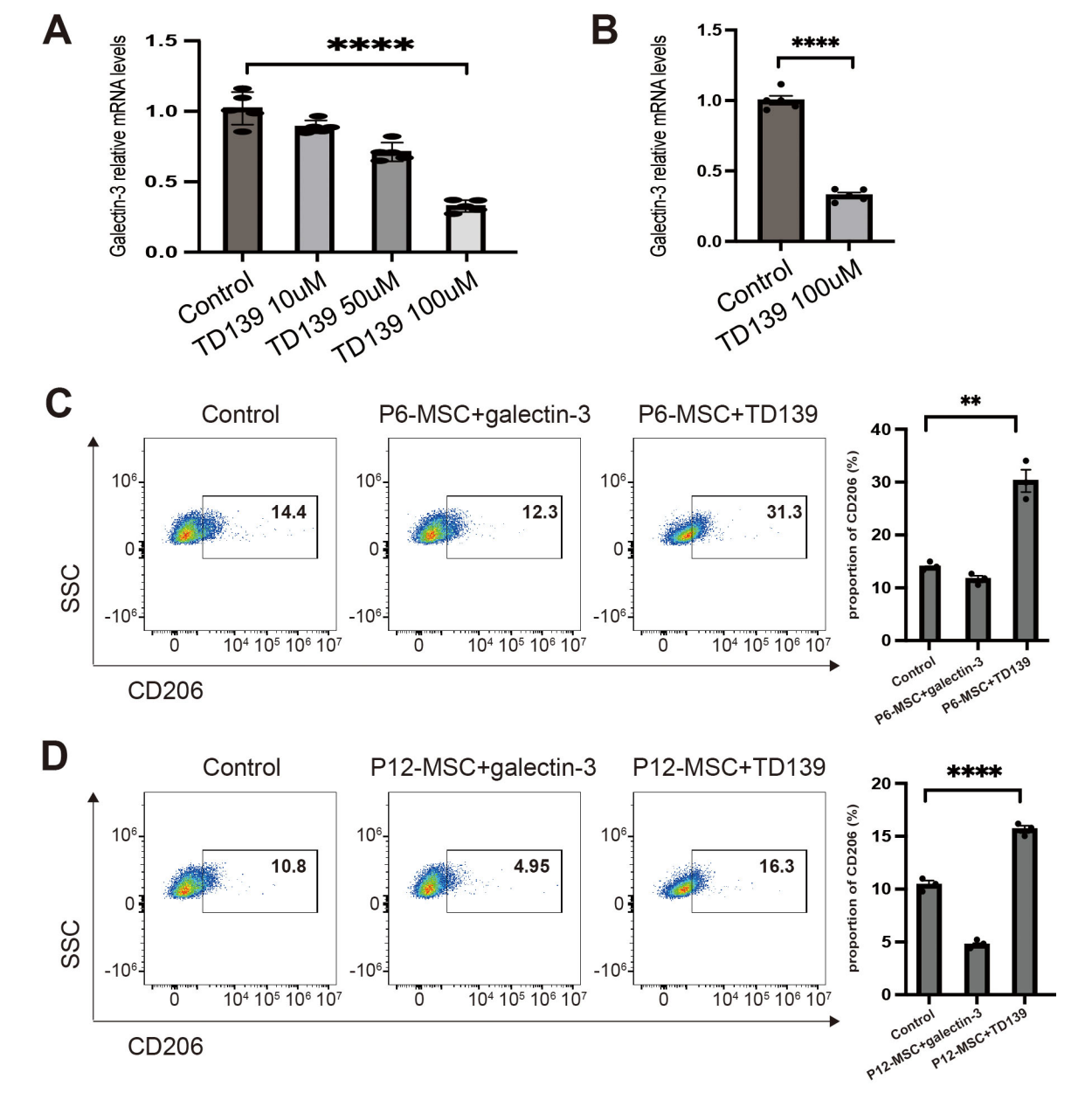


Fig. 6. The effect of TD139 on Gal-3 expression of MSCs and macrophage polarization induced by MSCs. MSCs at different passages were treated with DMSO, TD139 (10  $\mu$ M), TD139 (50  $\mu$ M) or TD139 (100  $\mu$ M) for 48 h (A,B). MSCs at different passages cocultured with Raw264.7 macrophages were treated with vehicle, Gal-3 (500 ng/mL) or TD139 (100  $\mu$ M) for 48 h (C,D). (A) qPCR analysis of Gal-3 expression in P12-MSCs. (B) qPCR analysis of Gal-3 expression in P6-MSCs. (C) Flow cytometry analysis of CD206<sup>+</sup> M2 macrophage proportion in Raw264.7 macrophages cocultured with P6-MSCs. (D) Flow cytometry analysis of CD206<sup>+</sup> M2 macrophage proportion in Raw264.7 macrophages cocultured with P12-MSCs. Data were pooled from 3 independent experiments. Data are presented as the mean  $\pm$  SD. \*\*p < 0.01, \*\*\*\*p < 0.0001.

enhances the immunoregulatory effect of MSCs at early passages on macrophages by promoting CD206<sup>+</sup> M2-like macrophages polarization. Furthermore, TD139 also saves the immunoregulatory function of MSCs at later passages via inducing CD206<sup>+</sup> M2-like macrophages polarization and suppressing iNOS<sup>+</sup> M1-like macrophages polarization. Additionally, both the proportion of CD206<sup>+</sup> M2-like macrophages and iNOS<sup>+</sup> M1-like macrophages rela-

tive to Raw264.7 macrophages in the TD139 treated P12-MSCs group was closely resembled the results observed in the TD139-treated P6-MSCs group. This indicated that TD139 treatment can restore the immunoregulatory capacity of MSCs at later passages to levels comparable to those at early passages, further confirming that TD139 can preserve the immunoregulatory function of MSCs at late passages.



### 4. Discussion

In the past few years, due to its immunosuppressive ability, MSCs have been applied for the treatment of GVHD after allo-HSCT, including gut GVHD, as well as for the management of refractory Crohn's disease [4,39–41]. MSCs derived from various biological sources usually require *ex vivo* expansion to achieve sufficient cell numbers for *in vivo* applications [14]. However, repeated *in vitro* passaging negatively affects the biological characteristics of MSCs, leading to a decline in their immunosuppressive and regenerative potential with each passage [16–18]. Therefore, it is necessary to develop strategies to save the immunosuppressive capability of MSCs during passaging, particularly for MSCs at later passage.

Several preclinical and clinical studies have documented the advantageous impacts of MSCs on GVHD [42– 44]. Nevertheless, other studies have shown that in vitro aging adversely affects the immunosuppressive function of MSCs. Gao et al.'s study [45] elucidated that MSCs undergo a progressive aging process in vitro, and the cellular senescence influences their immunosuppressive activity. Von Bahr et al. [46] reported that in GVHD patients, 1-year survival was 75% in patients who received earlypassage MSCs (from passages 1 to 2) in contrast to 21% in those who using later passage MSCs (from passages 3 to 4). In this study, we compared the therapeutic efficacy of MSCs at different passages in aGVHD mice model. Our data showed that compared to the control group, the severity of GVHD and tissue damage were not significantly different in the late-passage MSC group, whereas they were notably decreased in the early-passage MSC group, indicating that the therapeutic efficacy of MSCs diminishes with increasing passage.

In the pathogenesis of aGVHD, conditioning regimens in allo-HSCT initially activate host antigen-presenting cells, mainly macrophages and dendritic cells, thereby positioning macrophages as a central focus of research [34]. Previous studies have shown that with the progressive expansion in vitro, MSCs have undergone a phenotypic transformation from anti-inflammatory to pro-inflammatory, which leads to the deterioration of their therapeutic effects [47–49]. Thus, in this study, we examined peritoneal macrophages derived from aGVHD mice under various treatment. Consistent with previous studies, M2-like macrophages were increased in aGVHD mice treated with early-passage MSCs [50-52]. However, in contrast to the early-passage MSC treatment group, the number of M2-like macrophages was significantly reduced in the late-passage MSC group, suggesting that the variability in therapeutic efficacy of MSCs at different passages is associated with macrophage polarization. Subsequently, we conducted experiments with the Raw264.7 macrophage cell line, and the results showed that the effect of late-passage MSCs on M2-like macrophages polarization was notably weakened compared to early-passage MSCs. Taken together,

these results underscored the relationship between the immunomodulatory efficient of MSCs at different passages and macrophages polarization.

Gal-3 belongs to the beta-galactoside-binding animal lectin family, manifesting pleiotropic functions such as mediating cell-cell interactions, cell-matrix adhesion, and transmembrane signaling. It is produced by MSCs and exerts immunomodulatory effects [53]. Accumulating evidences have revealed that Gal-3 plays a pivotal role in macrophage polarization and the pathogenesis of aGVHD [37,54]. Li H et al. [54] provided evidence indicating that Gal-3 enhances inflammatory response by directly binding to NLRP3 in RAW264.7 macrophages. Therefore, we inferred that there may be an association between Gal-3, MSCs and macrophages. In the present study, we observed that Gal-3 expression was significantly increased in latepassage MSCs. Moreover, Gal-3 promoted an inflammatory response in Raw264.7 macrophages, notably by increasing M1-like macrophage polarization and expression of iNOS, IL-6, TNF- $\alpha$ , CCL2, CCL3, CCL4, COX2, while decreasing M2-like macrophage polarization and expression of CD206, IL-10, TGF- $\beta$ 1, Arg, Ym1. Collectively, these findings suggested that the reduced therapeutic efficacy of MSCs at late passages was related to the upregulation of Gal-3 expression. While telomere attrition and DNA damage are established drivers of replicative senescence in passaged MSCs, Gal-3 emerges as a distinct senescence inducer that functions independently of both telomeric erosion and DNA repair machinery [55–59].

TD139 has emerged as the foremost small molecule inhibitor targeting Gal-3 and has been extensively investigated in various experimental studies for its potential applications [60]. Currently, it represents a promising therapeutic agent for idiopathic pulmonary fibrosis in the phase II clinical trial [28]. Previous studies have underscored the therapeutic potential in lung fibrosis, cancer metastasis and hepatitis [61-63]. Here, we investigated the therapeutic role of TD139 in GVHD mice and its effects on MSCs for the first time. As shown in Supplementary Fig. 6, TD139 treatment in Raw 264.7 cells reduced the iNOS+ M1 macrophage population while increasing the CD206<sup>+</sup> M2 macrophage subset. This data indicated that TD139 directly inhibits M1-like macrophage polarization while promoting M2-like polarization. Nevertheless, as shown in Fig. 6, our results strongly indicated that TD139 dose-dependently suppressed the expression of Gal-3 in MSCs without affecting their biological properties. Inhibition of Gal-3 by TD139 significantly promoted M2-like macrophage polarization in both the P6-MSCs-Raw264.7 and P12-MSCs-Raw264.7 coculture systems, suggesting that TD139 enhanced the effect of MSCs on macrophages by inducing M2-like polarization. More importantly, in the presence of TD139, the proportion of M2-like macrophages was higher in Raw264.7 cells cocultured with P12-MSCs than in those cocultured with P6-MSCs. Although TD139 exhibited di-



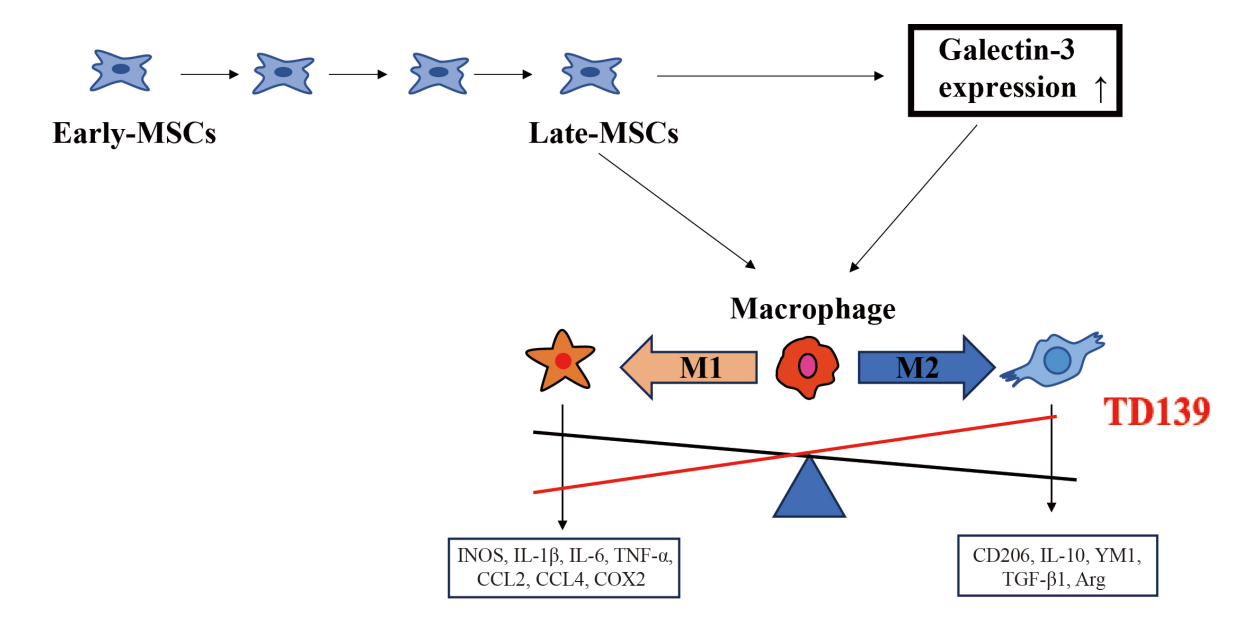


Fig. 7. The diagram of main results. MSCs, mesenchymal stem cells; IL-1 $\beta$ , interleukin 1b; IL-10, interleukin 10; IL-6, interleukin 6; COX2, cyclooxygenase 2; CCL2, CC-chemokine ligand 2; CCL4, CC-chemokine ligand 4; TGF- $\beta$ 1, Transforming growth factorbeta1; Arg, Arginase; TNF- $\alpha$ , Tumor necrosis factor- $\alpha$ ; iNOS, inducible nitric oxide synthase;  $\uparrow$ , the upward arrow indicated increased expression of galectin-3.

rect effects on macrophage polarization, its efficacy was substantially potentiated with the present of MSCs, suggesting that TD139 partially restored the immunomodulatory function of MSCs. Taken together, these findings suggested that TD139 can save the diminished immunoregulatory function of MSCs, particularly late-passage MSCs, enabling more MSCs to be obtained through passaging while preserving their immunoregulatory capabilities.

Although TD139-pretreated MSCs is a promising strategy for GVHD therapy, several challenges remain in their clinical application. We attempted to apply TD139 for pretreating MSCs and subsequently inject TD139pretreated MSCs into GVHD mice. However, the results were not satisfactory (data not shown). In our opinion, the following factors may contribute to this outcome: First, TD139 may not fully inhibit the expression of Gal-3 in MSCs. Second, after TD139 pretreatment of MSCs in vitro, the expression of Gal-3 in MSCs may recover in vivo. To address these issues, we plan to use small interfering RNA (siRNA) to inhibit the expression of Gal-3 in MSCs for a prolonged period in future studies. Additionally, we aim to apply TD139 and MSCs simultaneously, rather than pretreating MSCs with TD139. In addition, our data demonstrated that Gal-3 inhibited M2-like macrophage polarization, mechanistic details require further study. Prior evidence implicated Gal-3 in regulating macrophage function through NF-κB [64], TLR4/MyD88 [65], and CD98-PI3K pathways [66]. These pathways possibly mediate the M2like macrophage suppression, future work will include coimmunoprecipitation for receptor interactions and pathwayspecific inhibitors to elucidate signaling roles. Besides,

TD139's high polarity results in poor intestinal absorption necessitating alternative delivery routes [67]. Inhaled delivery of TD139, faces limitations in systemic diseases such as GVHD due to its dependency on patient adherence and inability to address extra-pulmonary manifestations [28]. To overcome these constraints, the next-generation galectin-3 inhibitor GB1211 was engineered for oral bioavailability, which maintains target affinity while enabling systemic exposure critical for GVHD therapy [67].

In conclusion, as shown in Fig. 7, the reduced therapeutic effect of late passage MSCs in treating GVHD is related to their impaired capacity to induce M2 macrophage polarization. Our study showed that the expression of Gal-3 increased in late passage MSCs, and that Gal-3 can suppress M2 macrophage polarization. Therefore, it is likely that Gal-3 plays a pivotal role in mediating the ability of MSCs to regulate macrophage polarization. Notably, treatment with TD139, a selective Gal-3 inhibitor, can restore the immunoregulatory function of late passage MSCs *in vitro*.

# 5. Conclusion

In summary, our study demonstrated that passaging *in vitro* impairs the therapeutic efficacy of MSCs in GVHD due to elevated Gal-3 expression in late-passage MSCs. Gal-3 directly suppressed M2-like macrophage polarization, thereby attenuating the immunoregulatory function of late-passage MSCs. TD139, a selective Gal-3 inhibitor, could restores the immunoregulatory function of MSCs, facilitating the clinical application of expanded MSCs for GVHD treatment.



### **Abbreviations**

MSCs, mesenchymal stem cells; allo-HSCT, Allogeneic hematopoietic stem cell transplantation; GVHD, graft versus host diseases; APCs, antigen-presenting cells; Gal-3, Galectin-3; LPS, lipopolysaccharide; IL-10, interleukin 10; IL-6, interleukin 6; COX2, cyclooxygenase 2; CCL2, CC-chemokine ligand 2; CCL3, CC-chemokine ligand 3; CCL4, CC-chemokine ligand 4; Arg, Arginase; IL-1 $\beta$ , interleukin 1 $\beta$ ; TNF- $\alpha$ , Tumor necrosis factor- $\alpha$ ; TGF- $\beta$ 1, Transforming growth factor-beta1; Th1, T helper 1; Th17, T helper 17; DMEM-L, Dulbecco modified Eagle medium-low glucose; DMEM, Dulbecco modified Eagle medium glucose; FBS, fetal bovine serum; P/S, penicillin-streptomycin; EDTA, ethylenediaminetetraacetic acid; Sca1, spinocerebellar ataxia type 1; FCM, flow cytometry; mAbs, monoclonal antibodies; PE, phycoerythrin; APC, allophycocyanin; FITC, Fluorescein isothiocyanate; PE-Cy7, R-Phycoerythrin-Cyanine 7; iNOS, inducible nitric oxide synthase; PBS, phosphate buffered solution; BM, bone marrow; BMT, bone marrow transplantation; TCD-BMC, T cell depleted-bone marrow cells; H&E, hematoxylin and eosin; CCK-8, Cell counting kit 8.

# Availability of Data and Materials

The raw data supporting the conclusions of this article will be made available by the authors, without undue reservation.

### **Author Contributions**

The concept was conceived by SGH. The overall study design was developed by MHW, JBW and SGH. The experiments were performed by MHW, FH, YJ, DFZ, and JBW. The data analysis was performed by MHW and YJ. The manuscript was written by MHW, JBW and SGH. The research was supervised by JBW and SGH. All authors contributed to editorial changes in the manuscript. All authors read and approved the final manuscript. All authors have participated sufficiently in the work and agreed to be accountable for all aspects of the work.

## **Ethics Approval and Consent to Participate**

The animal study was approved by the Ethics Committee of Xinhua Hospital Affiliated to the Shanghai Jiao Tong University School of Medicine (Ethics Approval No. XHEC-F-2022-076). All experimental procedures were performed in accordance with the 3R principle (Replacement, Reduction, and Refinement) for animal research, aiming to minimize animal suffering and optimize experimental design.

## Acknowledgment

Not applicable.

### **Funding**

This research received no external funding.

### **Conflict of Interest**

The authors declare no conflict of interest.

# **Supplementary Material**

Supplementary material associated with this article can be found, in the online version, at https://doi.org/10.31083/FBL39918.

#### References

- Shono Y, van den Brink MRM. Gut microbiota injury in allogeneic haematopoietic stem cell transplantation. Nature Reviews. Cancer. 2018; 18: 283–295. https://doi.org/10.1038/nrc. 2018.10.
- [2] Zeiser R, Blazar BR. Acute Graft-versus-Host Disease Biologic Process, Prevention, and Therapy. The New England Journal of Medicine. 2017; 377: 2167–2179. https://doi.org/10.1056/NEJMra1609337.
- [3] Blazar BR, Murphy WJ, Abedi M. Advances in graft-versushost disease biology and therapy. Nature Reviews. Immunology. 2012; 12: 443–458. https://doi.org/10.1038/nri3212.
- [4] Pittenger MF, Discher DE, Péault BM, Phinney DG, Hare JM, Caplan AI. Mesenchymal stem cell perspective: cell biology to clinical progress. NPJ Regenerative Medicine. 2019; 4: 22. http s://doi.org/10.1038/s41536-019-0083-6.
- [5] Wei X, Yang X, Han ZP, Qu FF, Shao L, Shi YF. Mesenchymal stem cells: a new trend for cell therapy. Acta Pharmacologica Sinica. 2013; 34: 747–754. https://doi.org/10.1038/aps.2013.50.
- [6] Le Blanc K, Mougiakakos D. Multipotent mesenchymal stromal cells and the innate immune system. Nature Reviews. Immunology. 2012; 12: 383–396. https://doi.org/10.1038/nri3209.
- [7] Ren G, Zhang L, Zhao X, Xu G, Zhang Y, Roberts AI, et al. Mesenchymal stem cell-mediated immunosuppression occurs via concerted action of chemokines and nitric oxide. Cell Stem Cell. 2008; 2: 141–150. https://doi.org/10.1016/j.stem.2007.11.014.
- [8] Shi Y, Wang Y, Li Q, Liu K, Hou J, Shao C, et al. Immunoregulatory mechanisms of mesenchymal stem and stromal cells in inflammatory diseases. Nature Reviews. Nephrology. 2018; 14: 493–507. https://doi.org/10.1038/s41581-018-0023-5.
- [9] Ma S, Xie N, Li W, Yuan B, Shi Y, Wang Y. Immunobiology of mesenchymal stem cells. Cell Death and Differentiation. 2014; 21: 216–225. https://doi.org/10.1038/cdd.2013.158.
- [10] Hsu WT, Lin CH, Chiang BL, Jui HY, Wu KKY, Lee CM. Prostaglandin E2 potentiates mesenchymal stem cell-induced IL-10+IFN-γ+CD4+ regulatory T cells to control transplant arteriosclerosis. Journal of Immunology (Baltimore, Md.: 1950). 2013; 190: 2372–2380. https://doi.org/10.4049/jimmun ol.1202996.
- [11] Hu J, Zhang L, Wang N, Ding R, Cui S, Zhu F, et al. Mesenchymal stem cells attenuate ischemic acute kidney injury by inducing regulatory T cells through splenocyte interactions. Kidney International. 2013; 84: 521–531. https://doi.org/10.1038/ki.2013.114.
- [12] In 't Anker PS, Scherjon SA, Kleijburg-van der Keur C, de Groot-Swings GMJS, Claas FHJ, Fibbe WE, et al. Isolation of mesenchymal stem cells of fetal or maternal origin from human placenta. Stem Cells (Dayton, Ohio). 2004; 22: 1338–1345. https://doi.org/10.1634/stemcells.2004-0058.
- [13] Zuk PA, Zhu M, Ashjian P, De Ugarte DA, Huang JI, Mizuno H, *et al.* Human adipose tissue is a source of multipotent stem



- cells. Molecular Biology of the Cell. 2002; 13: 4279–4295. https://doi.org/10.1091/mbc.e02-02-0105.
- [14] Kim M, Rhee JK, Choi H, Kwon A, Kim J, Lee GD, *et al.* Passage-dependent accumulation of somatic mutations in mesenchymal stromal cells during in vitro culture revealed by whole genome sequencing. Scientific Reports. 2017; 7: 14508. https://doi.org/10.1038/s41598-017-15155-5.
- [15] Hayashi Y, Yimiti D, Sanada Y, Ding C, Omoto T, Ogura T, et al. The therapeutic capacity of bone marrow MSC-derived extracellular vesicles in Achilles tendon healing is passage-dependent and indicated by specific glycans. FEBS Letters. 2022; 596: 1047–1058. https://doi.org/10.1002/1873-3468.14333.
- [16] Moravcikova E, Meyer EM, Corselli M, Donnenberg VS, Donnenberg AD. Proteomic Profiling of Native Unpassaged and Culture-Expanded Mesenchymal Stromal Cells (MSC). Cytometry. Part a: the Journal of the International Society for Analytical Cytology. 2018; 93: 894–904. https://doi.org/10.1002/cytoa.23574.
- [17] de Castro LL, Lopes-Pacheco M, Weiss DJ, Cruz FF, Rocco PRM. Current understanding of the immunosuppressive properties of mesenchymal stromal cells. Journal of Molecular Medicine (Berlin, Germany). 2019; 97: 605–618. https://doi.or g/10.1007/s00109-019-01776-y.
- [18] Ankrum JA, Dastidar RG, Ong JF, Levy O, Karp JM. Performance-enhanced mesenchymal stem cells via intracellular delivery of steroids. Scientific Reports. 2014; 4: 4645. https://doi.org/10.1038/srep04645.
- [19] Lorenzo-Almorós A, Pello A, Aceña Á, Martínez-Milla J, González-Lorenzo Ó, Tarín N, et al. Galectin-3 Is Associated with Cardiovascular Events in Post-Acute Coronary Syndrome Patients with Type-2 Diabetes. Journal of Clinical Medicine. 2020; 9: 1105. https://doi.org/10.3390/jcm9041105.
- [20] Dong R, Zhang M, Hu Q, Zheng S, Soh A, Zheng Y, et al. Galectin-3 as a novel biomarker for disease diagnosis and a target for therapy (Review). International Journal of Molecular Medicine. 2018; 41: 599–614. https://doi.org/10.3892/ijmm .2017.3311.
- [21] Radosavljevic G, Volarevic V, Jovanovic I, Milovanovic M, Pejnovic N, Arsenijevic N, et al. The roles of Galectin-3 in autoimmunity and tumor progression. Immunologic Research. 2012; 52: 100–110. https://doi.org/10.1007/s12026-012-8286-6.
- [22] Jia W, Kidoya H, Yamakawa D, Naito H, Takakura N. Galectin-3 accelerates M2 macrophage infiltration and angiogenesis in tumors. The American Journal of Pathology. 2013; 182: 1821–1831. https://doi.org/10.1016/j.ajpath.2013.01.017.
- [23] Liu Y, Zhao C, Meng J, Li N, Xu Z, Liu X, et al. Galectin-3 regulates microglial activation and promotes inflammation through TLR4/MyD88/NF-kB in experimental autoimmune uveitis. Clinical Immunology (Orlando, Fla.). 2022; 236: 108939. https://doi.org/10.1016/j.clim.2022.108939.
- [24] Xu GR, Zhang C, Yang HX, Sun JH, Zhang Y, Yao TT, *et al.* Modified citrus pectin ameliorates myocardial fibrosis and inflammation via suppressing galectin-3 and TLR4/MyD88/NFκB signaling pathway. Biomedicine & Pharmacotherapy =
  Biomedecine & Pharmacotherapie. 2020; 126: 110071. https://doi.org/10.1016/j.biopha.2020.110071.
- [25] Gilson RC, Gunasinghe SD, Johannes L, Gaus K. Galectin-3 modulation of T-cell activation: mechanisms of membrane remodelling. Progress in Lipid Research. 2019; 76: 101010. https://doi.org/10.1016/j.plipres.2019.101010.
- [26] Liu H, Hwang SY, Lee SS. Role of Galectin in Cardiovascular Conditions including Cirrhotic Cardiomyopathy. Pharmaceuticals (Basel, Switzerland). 2023; 16: 978. https://doi.org/10.3390/ph16070978.
- [27] Kumar A, Paul M, Panda M, Jayaram S, Kalidindi N, Sale H, et al. Molecular mechanism of interspecies differences in the

- binding affinity of TD139 to Galectin-3. Glycobiology. 2021; 31: 1390–1400. https://doi.org/10.1093/glycob/cwab072.
- [28] Hirani N, MacKinnon AC, Nicol L, Ford P, Schambye H, Pedersen A, et al. Target inhibition of galectin-3 by inhaled TD139 in patients with idiopathic pulmonary fibrosis. The European Respiratory Journal. 2021; 57: 2002559. https://doi.org/10.1183/13993003.02559-2020.
- [29] Ren Z, Yu P, Li D, Li Z, Liao Y, Wang Y, et al. Single-Cell Reconstruction of Progression Trajectory Reveals Intervention Principles in Pathological Cardiac Hypertrophy. Circulation. 2020; 141: 1704–1719. https://doi.org/10.1161/CIRCULATIO NAHA.119.043053.
- [30] Chen Y, Fu W, Zheng Y, Yang J, Liu Y, Qi Z, et al. Galectin 3 enhances platelet aggregation and thrombosis via Dectin-1 activation: a translational study. European Heart Journal. 2022; 43: 3556–3574. https://doi.org/10.1093/eurheartj/ehac034.
- [31] Gordon S, Martinez FO. Alternative activation of macrophages: mechanism and functions. Immunity. 2010; 32: 593–604. https://doi.org/10.1016/j.immuni.2010.05.007.
- [32] Lawrence T, Natoli G. Transcriptional regulation of macrophage polarization: enabling diversity with identity. Nature Reviews. Immunology. 2011; 11: 750–761. https://doi.org/10.1038/nr i3088
- [33] Hou P, Fang J, Liu Z, Shi Y, Agostini M, Bernassola F, et al. Macrophage polarization and metabolism in atherosclerosis. Cell Death & Disease. 2023; 14: 691. https://doi.org/10.1038/s41419-023-06206-z.
- [34] Wu K, Yuan Y, Yu H, Dai X, Wang S, Sun Z, et al. The gut microbial metabolite trimethylamine N-oxide aggravates GVHD by inducing M1 macrophage polarization in mice. Blood. 2020; 136: 501–515. https://doi.org/10.1182/blood.2019003990.
- [35] Rashidi A, DiPersio JF, Sandmaier BM, Colditz GA, Weisdorf DJ. Steroids Versus Steroids Plus Additional Agent in Frontline Treatment of Acute Graft-versus-Host Disease: A Systematic Review and Meta-Analysis of Randomized Trials. Biology of Blood and Marrow Transplantation: Journal of the American Society for Blood and Marrow Transplantation. 2016; 22: 1133–1137. https://doi.org/10.1016/j.bbmt.2016.02.021.
- [36] Sioud M. New insights into mesenchymal stromal cell-mediated T-cell suppression through galectins. Scandinavian Journal of Immunology. 2011; 73: 79–84. https://doi.org/10.1111/j. 1365-3083.2010.02491.x.
- [37] McCarthy PL, Attwood KM, Liu X, Chen GL, Minderman H, Alousi A, et al. Galectin-3 predicts acute GvHD and overall mortality post reduced intensity allo-HCT: a BMT-CTN biorepository study. Bone Marrow Transplantation. 2024; 59: 334–343. https://doi.org/10.1038/s41409-023-02168-0.
- [38] Lederer DJ, Martinez FJ. Idiopathic Pulmonary Fibrosis. The New England Journal of Medicine. 2018; 379: 797–798. https://doi.org/10.1056/NEJMc1807508.
- [39] Duijvestein M, Vos ACW, Roelofs H, Wildenberg ME, Wendrich BB, Verspaget HW, *et al.* Autologous bone marrowderived mesenchymal stromal cell treatment for refractory luminal Crohn's disease: results of a phase I study. Gut. 2010; 59: 1662–1669. https://doi.org/10.1136/gut.2010.215152.
- [40] Müller I, Kordowich S, Holzwarth C, Isensee G, Lang P, Neunhoeffer F, et al. Application of multipotent mesenchymal stromal cells in pediatric patients following allogeneic stem cell transplantation. Blood Cells, Molecules & Diseases. 2008; 40: 25–32. https://doi.org/10.1016/j.bcmd.2007.06.021.
- [41] Ringdén O, Uzunel M, Sundberg B, Lönnies L, Nava S, Gustafsson J, et al. Tissue repair using allogeneic mesenchymal stem cells for hemorrhagic cystitis, pneumomediastinum and perforated colon. Leukemia. 2007; 21: 2271–2276. https://doi.org/10.1038/sj.leu.2404833.
- [42] Jang YK, Kim M, Lee YH, Oh W, Yang YS, Choi SJ. Optimiza-



- tion of the therapeutic efficacy of human umbilical cord blood-mesenchymal stromal cells in an NSG mouse xenograft model of graft-versus-host disease. Cytotherapy. 2014; 16: 298–308. https://doi.org/10.1016/j.jcyt.2013.10.012.
- [43] Kebriaei P, Isola L, Bahceci E, Holland K, Rowley S, McGuirk J, et al. Adult human mesenchymal stem cells added to corticosteroid therapy for the treatment of acute graft-versus-host disease. Biology of Blood and Marrow Transplantation: Journal of the American Society for Blood and Marrow Transplantation. 2009; 15: 804–811. https://doi.org/10.1016/j.bbmt.2008.03.012.
- [44] Le Blanc K, Rasmusson I, Sundberg B, Götherström C, Hassan M, Uzunel M, et al. Treatment of severe acute graft-versus-host disease with third party haploidentical mesenchymal stem cells. Lancet (London, England). 2004; 363: 1439–1441. https://doi.org/10.1016/S0140-6736(04)16104-7.
- [45] Gao Y, Chi Y, Chen Y, Wang W, Li H, Zheng W, et al. Multiomics analysis of human mesenchymal stem cells shows cell aging that alters immunomodulatory activity through the down-regulation of PD-L1. Nature Communications. 2023; 14: 4373. https://doi.org/10.1038/s41467-023-39958-5.
- [46] von Bahr L, Sundberg B, Lönnies L, Sander B, Karbach H, Hägglund H, et al. Long-term complications, immunologic effects, and role of passage for outcome in mesenchymal stromal cell therapy. Biology of Blood and Marrow Transplantation: Journal of the American Society for Blood and Marrow Transplantation. 2012; 18: 557–564. https://doi.org/10.1016/j.bbmt.2011.07.023.
- [47] Zhang Y, Ravikumar M, Ling L, Nurcombe V, Cool SM. Age-Related Changes in the Inflammatory Status of Human Mesenchymal Stem Cells: Implications for Cell Therapy. Stem Cell Reports. 2021; 16: 694–707. https://doi.org/10.1016/j.stemcr.2021.01.021.
- [48] Miclau K, Hambright WS, Huard J, Stoddart MJ, Bahney CS. Cellular expansion of MSCs: Shifting the regenerative potential. Aging Cell. 2023; 22: e13759. https://doi.org/10.1111/acel.13759.
- [49] Hughes AM, Kuek V, Oommen J, Kotecha RS, Cheung LC. Murine bone-derived mesenchymal stem cells undergo molecular changes after a single passage in culture. Scientific Reports. 2024; 14: 12396. https://doi.org/10.1038/s41598-024-63009-8.
- [50] Bouchlaka MN, Moffitt AB, Kim J, Kink JA, Bloom DD, Love C, et al. Human Mesenchymal Stem Cell-Educated Macrophages Are a Distinct High IL-6-Producing Subset that Confer Protection in Graft-versus-Host-Disease and Radiation Injury Models. Biology of Blood and Marrow Transplantation: Journal of the American Society for Blood and Marrow Transplantation. 2017; 23: 897–905. https://doi.org/10.1016/j.bbmt 2017.02.018
- [51] Wu R, Liu C, Deng X, Chen L, Hao S, Ma L. Enhanced alleviation of aGVHD by TGF-β1-modified mesenchymal stem cells in mice through shifting MΦ into M2 phenotype and promoting the differentiation of Treg cells. Journal of Cellular and Molecular Medicine. 2020; 24: 1684–1699. https://doi.org/10.1111/jcmm.14862.
- [52] Chen B, Ni Y, Liu J, Zhang Y, Yan F. Bone Marrow-Derived Mesenchymal Stem Cells Exert Diverse Effects on Different Macrophage Subsets. Stem Cells International. 2018; 2018: 8348121. https://doi.org/10.1155/2018/8348121.
- [53] Yang RY, Rabinovich GA, Liu FT. Galectins: structure, function and therapeutic potential. Expert Reviews in Molecular Medicine. 2008; 10: e17. https://doi.org/10.1017/S1462399408000719.

- [54] Li H, Xiao L, He H, Zeng H, Liu J, Jiang C, et al. Quercetin Attenuates Atherosclerotic Inflammation by Inhibiting Galectin-3-NLRP3 Signaling Pathway. Molecular Nutrition & Food Research. 2021; 65: e2000746. https://doi.org/10.1002/mnfr.202000746.
- [55] Redaelli S, Bentivegna A, Foudah D, Miloso M, Redondo J, Riva G, et al. From cytogenomic to epigenomic profiles: monitoring the biologic behavior of in vitro cultured human bone marrow mesenchymal stem cells. Stem Cell Research & Therapy. 2012; 3: 47. https://doi.org/10.1186/scrt138.
- [56] Kipling D, Wynford-Thomas D, Jones CJ, Akbar A, Aspinall R, Bacchetti S, et al. Telomere-dependent senescence. Nature Biotechnology. 1999; 17: 313–314. https://doi.org/10.1038/7827.
- [57] Ferrucci L, Fabbri E. Inflammageing: chronic inflammation in ageing, cardiovascular disease, and frailty. Nature Reviews. Cardiology. 2018; 15: 505–522. https://doi.org/10.1038/ s41569-018-0064-2.
- [58] Clark MC, Pang M, Hsu DK, Liu FT, de Vos S, Gascoyne RD, et al. Galectin-3 binds to CD45 on diffuse large B-cell lymphoma cells to regulate susceptibility to cell death. Blood. 2012; 120: 4635–4644. https://doi.org/10.1182/blood-2012-06-438234.
- [59] Al-Azab M, Safi M, Idiiatullina E, Al-Shaebi F, Zaky MY. Aging of mesenchymal stem cell: machinery, markers, and strategies of fighting. Cellular & Molecular Biology Letters. 2022; 27: 69. https://doi.org/10.1186/s11658-022-00366-0.
- [60] St-Gelais J, Denavit V, Giguère D. Efficient synthesis of a galectin inhibitor clinical candidate (TD139) using a Payne rearrangement/azidation reaction cascade. Organic & Biomolecular Chemistry. 2020; 18: 3903–3907. https://doi.org/10.1039/d0o b00910e.
- [61] Lee JJ, Hsu YC, Li YS, Cheng SP. Galectin-3 Inhibitors Suppress Anoikis Resistance and Invasive Capacity in Thyroid Cancer Cells. International Journal of Endocrinology. 2021; 2021: 5583491. https://doi.org/10.1155/2021/5583491.
- [62] Volarevic V, Milovanovic M, Ljujic B, Pejnovic N, Arsenijevic N, Nilsson U, et al. Galectin-3 deficiency prevents concanavalin A-induced hepatitis in mice. Hepatology (Baltimore, Md.). 2012; 55: 1954–1964. https://doi.org/10.1002/hep.25542.
- [63] Mackinnon AC, Gibbons MA, Farnworth SL, Leffler H, Nilsson UJ, Delaine T, et al. Regulation of transforming growth factor-β1-driven lung fibrosis by galectin-3. American Journal of Respiratory and Critical Care Medicine. 2012; 185: 537–546. https://doi.org/10.1164/rccm.201106-0965OC.
- [64] Pei C, Zhang Y, Wang P, Zhang B, Fang L, Liu B, *et al.* Berberine alleviates oxidized low-density lipoprotein-induced macrophage activation by downregulating galectin-3 via the NF-kB and AMPK signaling pathways. Phytotherapy Research: PTR. 2019; 33: 294–308. https://doi.org/10.1002/ptr.6217.
- [65] Wang G, Li R, Feng C, Li K, Liu S, Fu Q. Galectin-3 is involved in inflammation and fibrosis in arteriogenic erectile dysfunction via the TLR4/MyD88/NF-κB pathway. Cell Death Discovery. 2024; 10: 92. https://doi.org/10.1038/s41420-024-01859-x.
- [66] Wang Z, Gao Z, Zheng Y, Kou J, Song D, Yu X, et al. Melatonin inhibits atherosclerosis progression via galectin-3 downregulation to enhance autophagy and inhibit inflammation. Journal of Pineal Research. 2023; 74: e12855. https://doi.org/10.1111/jpi. 12855
- [67] Zetterberg FR, MacKinnon A, Brimert T, Gravelle L, Johnsson RE, Kahl-Knutson B, et al. Discovery and Optimization of the First Highly Effective and Orally Available Galectin-3 Inhibitors for Treatment of Fibrotic Disease. Journal of Medicinal Chemistry. 2022; 65: 12626–12638. https://doi.org/10.1021/acs.jmedchem.2c00660.

